

Hierarchical Hollow-on-hollow NiCoP Electrocatalyst for Efficient Hydrogen Evolution Reaction

Supporting Information

Juntao Zhang ^{a,b}, Lipeng Zhang ^{a,b}, Xingdong Wang ^{a,b}, Wei Zhu ^{a,b,}, Zhongbin Zhuang ^{a,b,c*}*

^a State Key Lab of Organic-Inorganic Composites, Beijing University of Chemical Technology, Beijing 100029, China.

^b Beijing Advanced Innovation Center for Soft Matter Science and Engineering, Beijing University of Chemical Technology, Beijing 100029, China.

^c Beijing Key Laboratory of Energy Environmental Catalysis, Beijing University of Chemical Technology, Beijing 100029, China.

Experimental Section

Chemicals.

Cobaltous nitrate hexahydrate ($\text{Co}(\text{NO}_3)_2 \cdot 6\text{H}_2\text{O}$; A.R.; Sinopharm Chemical Reagent Co., Ltd., China), nickel(II) nitrate hexahydrate ($\text{Ni}(\text{NO}_3)_2 \cdot 6\text{H}_2\text{O}$; A.R.; Sinopharm Chemical Reagent Co., Ltd., China), 2-methylimidazole ($\text{C}_4\text{H}_6\text{N}_2$; A.R.; Sinopharm Chemical Reagent Co., Ltd., China), methanol (CH_3OH ; A.R.; Beijing Chemical Reagent Factory, China), ethanol ($\text{C}_2\text{H}_5\text{OH}$; A.R.; Beijing Chemical Reagent Factory, China), sulfuric acid (H_2SO_4 ; A.R.; Beijing Chemical Reagent Factory, China), platinum on carbon black (20 wt.% Pt/C; HISPEC-3000; Alfa Aesar), sodium hypophosphite (NaH_2PO_2 ; 99.0%; Aladdin). All chemical reagents were used without any further purification. Deionized water (18.2 $\text{M}\Omega \cdot \text{cm}$ resistivity) was used for all the electrochemical experiments.

Synthetic Methods.

Synthesis of ZIF-67. In a typical synthesis of ZIF-67, 3.28 g of 2-methylimidazole and 2.9 g of $\text{Co}(\text{NO}_3)_2 \cdot 6\text{H}_2\text{O}$ was dissolved in 100 mL of methanol, respectively. Then, the $\text{Co}(\text{NO}_3)_2 \cdot 6\text{H}_2\text{O}$ methanol solution was poured into the 2-methylimidazole solution, and the solution was stirred for 12 h. The product was collected by centrifugation and washed by methanol for three times.

Synthesis of ZIF-67@NiCo-LDH. 40 mg of ZIF-67 was dispersed in 20 mL of ethanol, and 90 mg of $\text{Ni}(\text{NO}_3)_2 \cdot 6\text{H}_2\text{O}$ was dissolved in 5 mL of ethanol. Then, the ZIF-67 dispersion was added into the $\text{Ni}(\text{NO}_3)_2 \cdot 6\text{H}_2\text{O}$ solution, and the solution was stirred for different times. Finally, the product was collected by centrifugation, and washed by methanol for three times.

Synthesis of NiCo. The NiCo was obtained by the high-temperature pyrolysis of ZIF-67@NiCo-LDH at 900 °C for 2 h with a heating rate of 5 °C·min⁻¹. The pyrolysis was conducted in a tubular furnace equipped with a programmed temperature controller by using N_2 as the protective atmosphere.

Synthesis of HiHo-NiCoP. The as-obtained NiCo (about 10 mg) and NaH_2PO_2 (1 g) were placed in two separated porcelain boats in the tubular furnace, and the NiCo was placed at the upstream. Then the quartz tube was heated up to 300 °C with a heating rate of 5 °C·min⁻¹. N_2 was used as the protective atmosphere in the phosphidation.

Synthesis of NiCo-ZIF-67. The synthesis method for NiCo-ZIF-67 was the same as that of ZIF-67 except adding 0.144 g of $\text{Ni}(\text{NO}_3)_2 \cdot 6\text{H}_2\text{O}$ into the $\text{Co}(\text{NO}_3)_2$ solution.

Synthesis of NiCoP NPs. 40 mg of NiCo-ZIF-67 and 1 g of NaH_2PO_2 were placed at two separate positions in a tubular furnace, and NaH_2PO_2 was at the upstream. Then the tubular furnace was heated up to 300 °C for 2 h with a heat rate of 5 °C min⁻¹ in N_2 atmosphere (>99.999%).

Synthesis of H1-NiCoP. The synthesis method for H1-NiCoP was the same as NiCoP NPs except using ZIF-67@NiCo-LDH as the precursor for the phosphidation.

Synthesis of H2-NiCoP. H2-NiCoP was obtained by the pyrolysis and phosphidation of NiCo-ZIF-67 under the same conditions as the synthesis of HiHo-NiCoP.

Synthesis of CoP. The synthesis method for CoP was the same as HiHo-NiCoP except using ZIF-67 as the precursor.

Synthesis of NiP. The NiP NPs were prepared by a modified phosphidation method.^[S1] 30 mg of $\text{Ni}(\text{NO}_3)_2 \cdot 6\text{H}_2\text{O}$ powder and 1 g of NaH_2PO_2 were placed in two separated porcelain boats in the tubular furnace, and $\text{Ni}(\text{NO}_3)_2 \cdot 6\text{H}_2\text{O}$ was placed at the upstream. Then the quartz tube was heated up to 300 °C with a heating rate of 5 °C·min⁻¹. N_2 was used as the protective atmosphere in the phosphidation.

Characterizations

XRD measurements were performed on a Bruker D8 diffractometer with Cu K α radiation ($\lambda=0.15406$ nm). TEM characterization was conducted on an FEI Tecnai G2 20m microscope at accelerating voltage of 200 kV. TEM samples were prepared by drop-casting the sample suspensions onto the copper grids with carbon films. HRTEM, EDS, and HAADF-STEM were performed on a JEOL JEM-2010F microscope with an accelerating voltage of 200 kV. XPS was conducted on the Thermo Fisher ESCALAB 250Xi analyzer with a monochromatic Al K α as the X-ray source.

Electrochemical Test

2.0 mg of the NiCoP catalysts were dispersed in a mixed solution consisted of 380 μL of H_2O , 100 μL of ethanol and 20 μL of 5 wt % Nafion. The suspensions were ultrasonicated for 1 h to prepare homogeneous ink solutions. Then 20 μL of the ink solution was dropwise added onto a glassy carbon

electrode ($d=5$ mm), resulting a mass loading of 0.41 mg cm^{-2} on the working electrode. The electrochemical measurements were conducted with an electrochemical workstation (CHI 660E) by using the typical three-electrode configuration, where a graphite rod was used as the counter electrode and a saturated calomel electrode (SCE) was used as the reference electrode. All the electrochemical measurements were tested in H_2 -saturated $0.5\text{M H}_2\text{SO}_4$ electrolyte. All the potentials in the text were referred to the reversible hydrogen electrode (RHE). The zero point of RHE was calibrated using the equilibrium potential of HOR/HER of Pt/C catalyst in H_2 -saturated H_2SO_4 electrolyte. iR compensation was employed to correct iR -drop for the HER polarization curves.

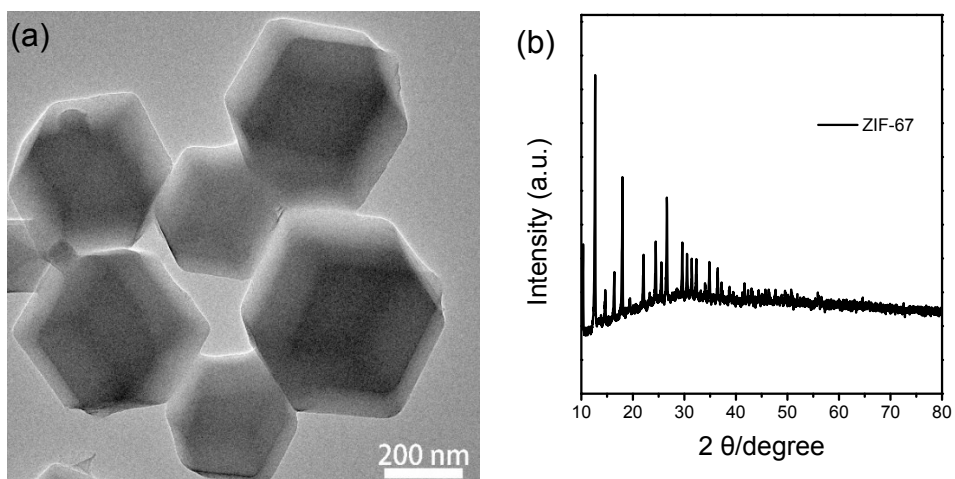


Figure S1 (a) TEM image and (b) XRD pattern of ZIF-67

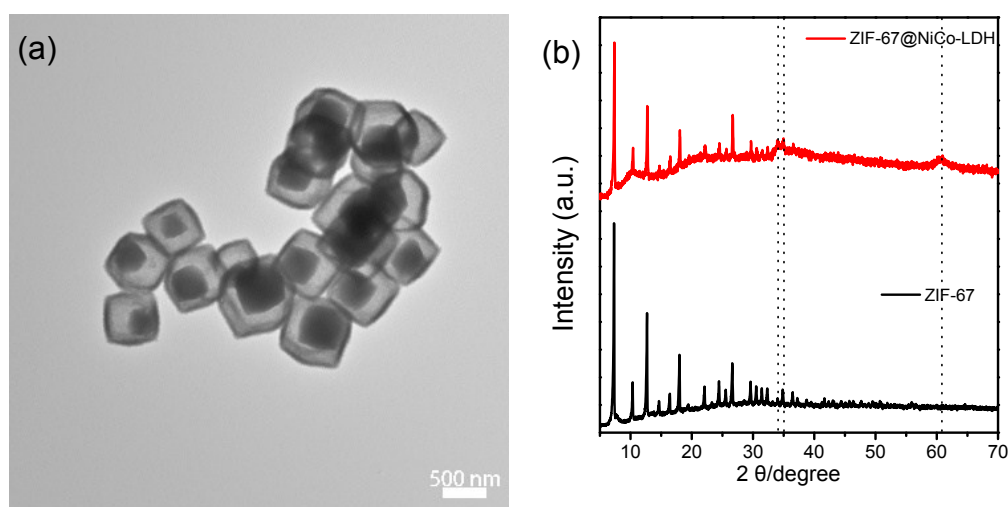


Figure S2 (a) TEM image and (b) XRD pattern of ZIF-67@NiCo-LDH. The TEM image of the product in Fig. S2a shows that the solid polyhedrons convert into yolk-shell structures of a larger size. Broad diffraction peaks at 10.51, 34.51, and 60.51 newly formed in the XRD pattern of the yolk-shell structures, as shown in Fig. S2b. These peaks were ascribed to the formation of NiCo layered double hydroxide shell structures (denoted as NiCo-LDH, I in Scheme 1) according to the reports regarding the synthesis of Ni-Co MOF derivatives.

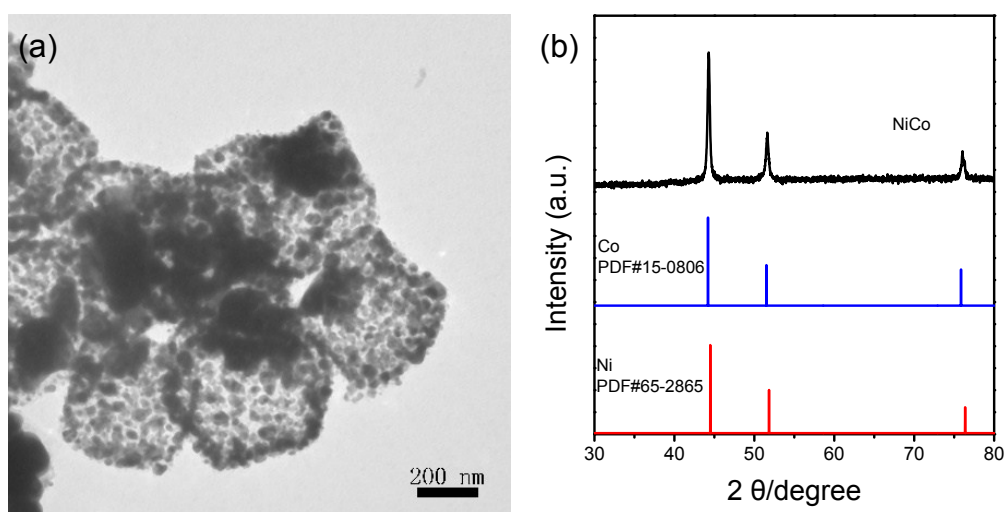


Figure S3 (a) TEM image and (b) XRD pattern of NiCo. The TEM image in Fig. S3a shows that hollow NiCo structures were assembled by many cross-linked NPs. The XRD pattern in Fig. S3b demonstrated that the NiCo NPs were in metallic status. In other words, both Ni^{2+} and Co^{2+} were reduced back to metals by the HMIM ligands during the high-temperature pyrolysis step.

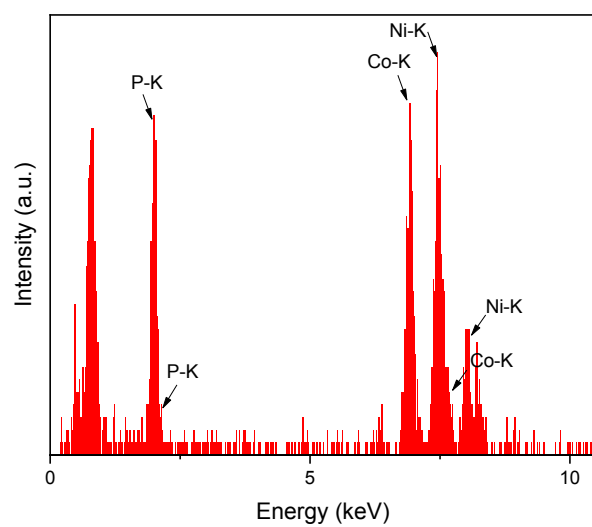


Figure S4 the EDS spectrum of the HiHo-NiCoP

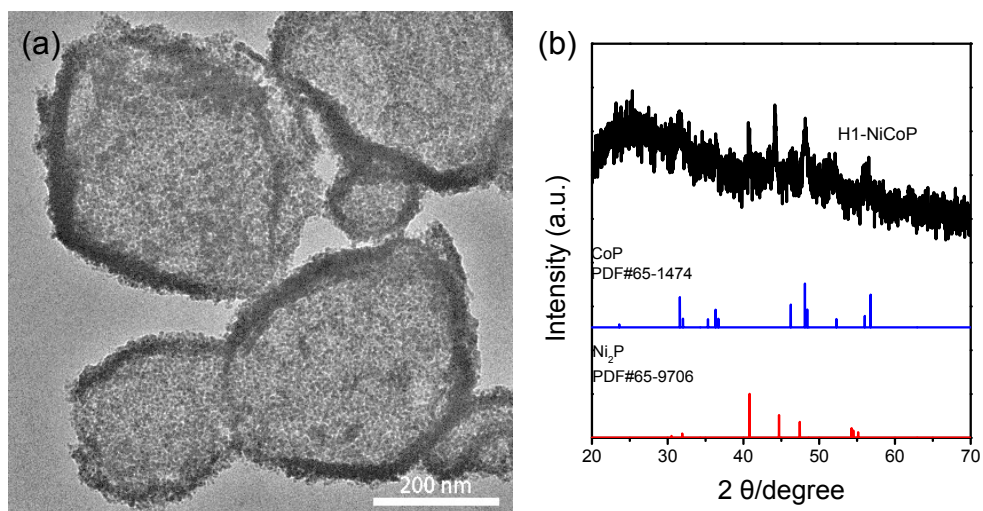


Figure S5 (a) TEM image and (b) XRD pattern of H1-NiCoP

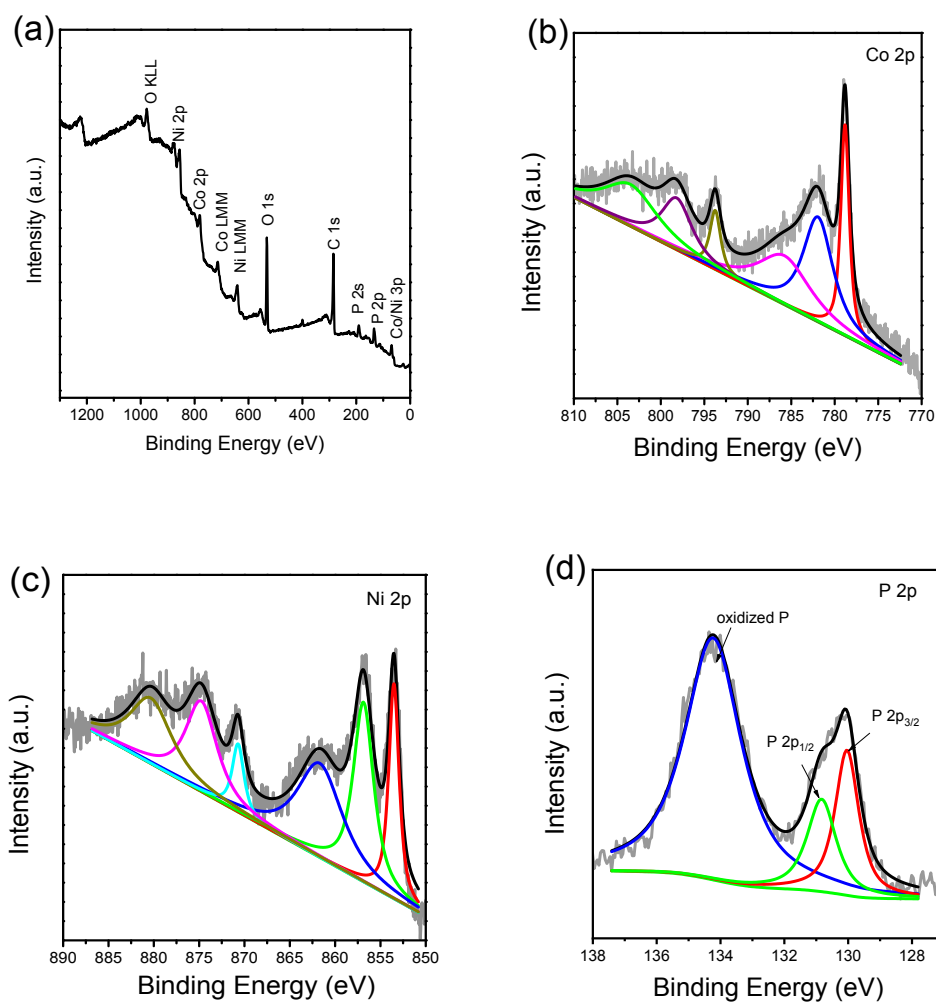


Figure S6 XPS spectra of HiHo-NiCoP: (a) survey scan, (b) Co 2p spectrum, (c) Ni 2p spectrum, (d) P 2p spectrum. The survey spectrum confirmed that the HiHo-NiCoP consisted of Co, Ni, P, C, N, and O on the surface (Fig. S6a). Phosphide took up 20.1% of the phosphorus species. XPS results confirmed the formation of metal phosphides on the surface, which is active for the HER.

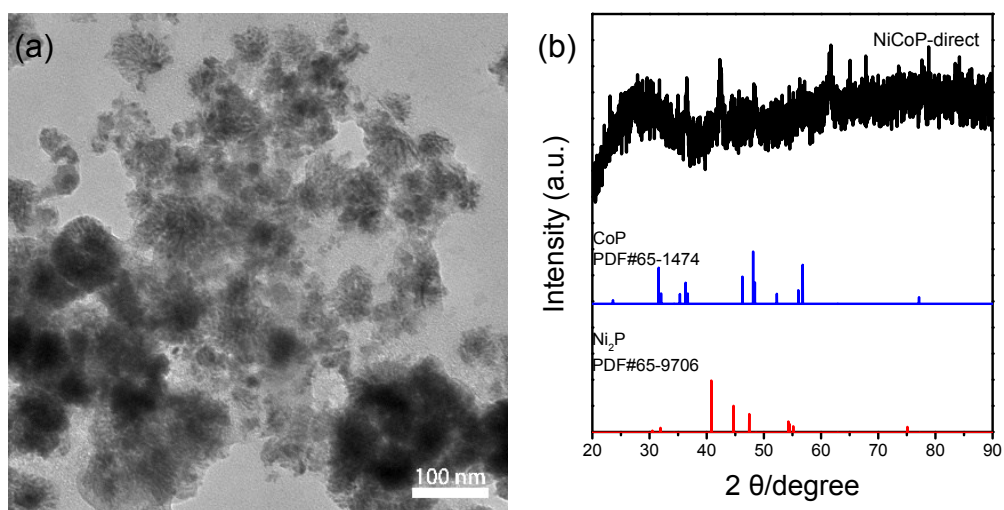


Figure S7 (a) TEM image and (b) XRD pattern of NiCoP nanoparticles

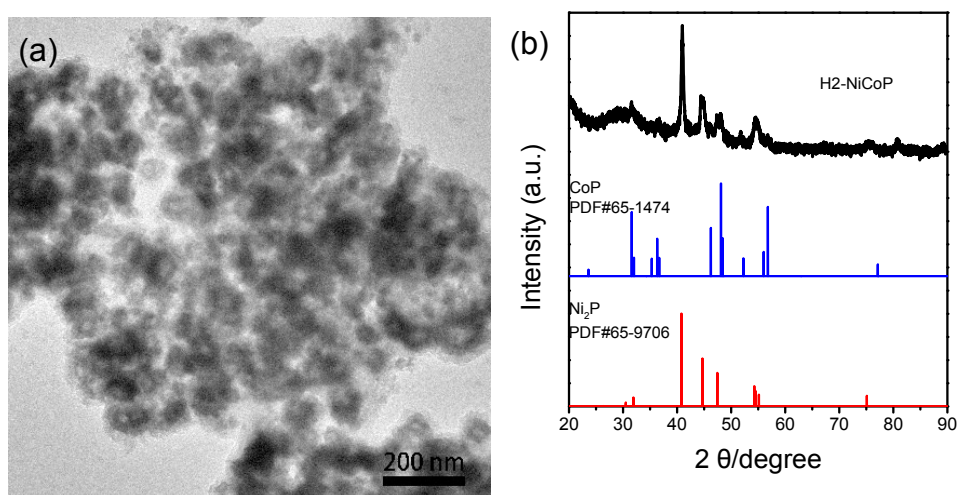


Figure S8 (a) TEM image and (b) XRD pattern of H2-NiCoP

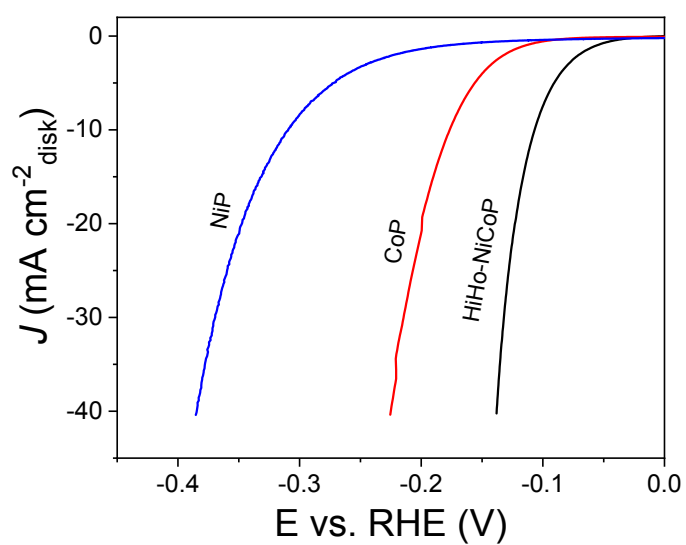


Figure S9 the HER polarization curves of the monometallic phosphide NPs obtained in 0.5 M H_2SO_4 with a scan rate of 5 mV s^{-1} .

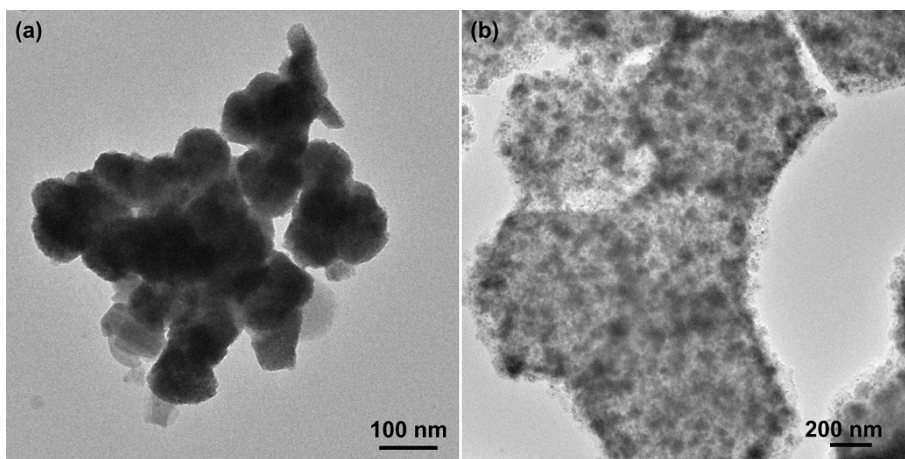


Figure S10 TEM images of (a) NiP NPs and (b) CoP NPs.

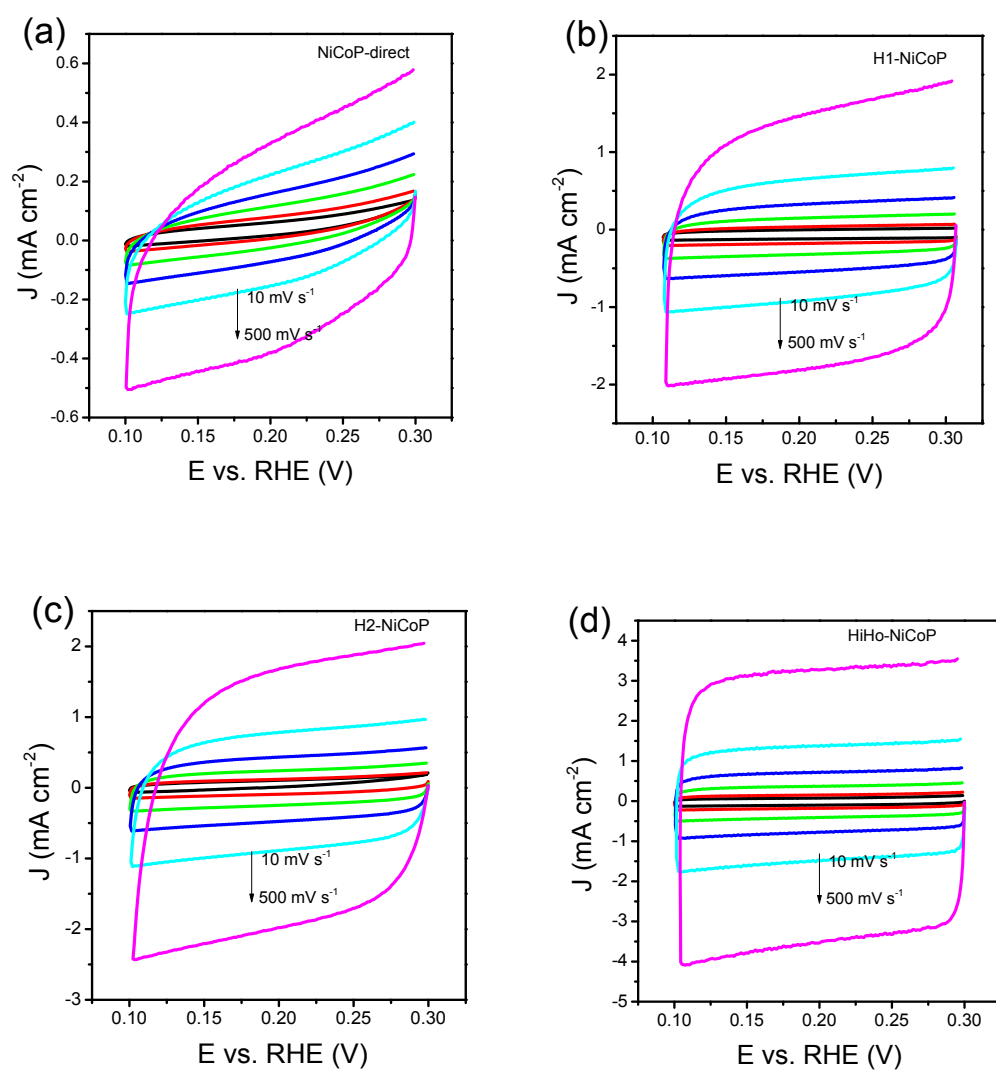


Figure S11 The polarization curves in the non-faradic region at different sweep rates: (a) NiCoP nanoparticle (solid), (b) H1-NiCoP, (c) H2-NiCoP, and (d) HiHo-NiCoP.

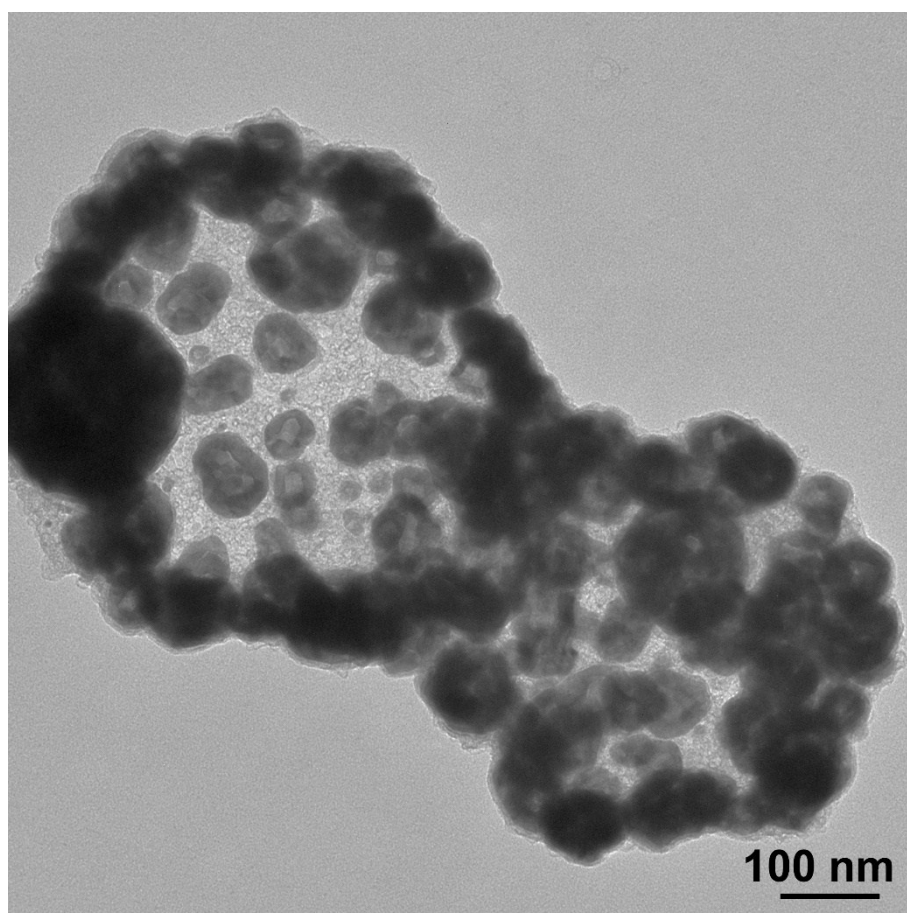


Figure S12 TEM image of the HiHo-NiCoP after the durability test.

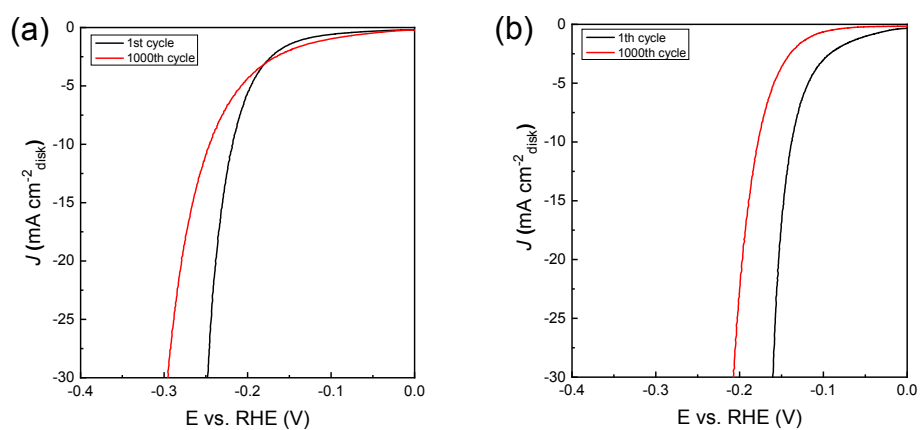


Figure S13 The HER polarization curves of (1) H1-NiCoP and (2) H2-NiCoP catalysts before and after ADT, i.e., 1000 cycles' CV scans between 0 and -0.2 V at a sweep rate of 50 mV·s⁻¹.

Table S1 Summary of the catalytic performance of the reported NiCoP electrocatalysts toward HER in 0.5 M H₂SO₄ electrolyte.

Catalysts	Ni:Co:P (atomic)	Loading (mg·cm ⁻²)	η_{10} (mV)	Tafel Slope (mV·dec ⁻¹)	Stability	Ref.
Co _{1.6} Ni _{0.4} P/CNTs	16:48:36	0.2	165	47	η_{10} increased 13 mV after 1000 cycles' ADT	[S2]
Ni-Co ₂ P/NCNTs	11:55:34	0.2	230	105	η_{10} unchanged after 1000 cycles' ADT	[S3]
Ni ₂ P/NiCoP@NCCs	32:18:50	0.5	120	90	η_{10} unchanged after 1000 cycles' ADT	[S4]
NiCoP/NF	NA	5.6	118	68	η_{10} unchanged after 1000 cycles' ADT	[S5]
Ni-Co-P/C60	NA	0.35	97	48	η_{10} increased 13 mV after 1000 cycles' ADT	[S6]
Co ₁ Ni ₁ -P@C	Ni:Co=1:1	0.5	169	73	η_{10} increased 25 mV after 5000 cycles' ADT	[S7]
HiHo-NiCoP	33:31:36	0.41	103	52	η_{10} unchanged after 5000 cycles' ADT	This work

Reference:

- [S1] L. Feng, H. Vrubel, M. Bensimon, X. Hu, Easily-prepared dinickel phosphide (Ni₂P) nanoparticles as an efficient and robust electrocatalyst for hydrogen evolution, *Phys. Chem. Chem. Phys.*, 16 (2014) 5917-5921.
- [S2] Y. Pan, Y. Chen, Y. Lin, P. Cui, K. Sun, Y. Liu, C. Liu, Cobalt nickel phosphide nanoparticles decorated carbon nanotubes as advanced hybrid catalysts for hydrogen evolution, *Journal of Materials Chemistry A*, 4 (2016) 14675-14686.
- [S3] Y. Pan, Y. Liu, Y. Lin, C. Liu, Metal Doping Effect of the M-Co₂P/Nitrogen-Doped Carbon Nanotubes (M = Fe, Ni, Cu) Hydrogen Evolution Hybrid Catalysts, *ACS Applied Materials & Interfaces*, 8 (2016) 13890-13901.
- [S4] L. Han, T.W. Yu, W. Lei, W.W. Liu, K. Feng, Y.L. Ding, G.P. Jiang, P. Xu, Z.W. Chen, Nitrogen-doped carbon nanocones encapsulating with nickel-cobalt mixed phosphides for enhanced hydrogen evolution reaction, *Journal of Materials Chemistry A*, 5 (2017) 16568-16572.
- [S5] T. Liu, X.Y. Yan, P.X. Xi, J. Chen, D.D. Qin, D.L. Shan, S. Devaramani, X.Q. Lu, Nickel-Cobalt phosphide nanowires supported on Ni foam as a highly efficient catalyst for electrochemical hydrogen evolution reaction, *International Journal of Hydrogen Energy*, 42 (2017) 14124-14132.
- [S6] Z.L. Du, N. Jannatun, D.Y. Yu, J. Ren, W.H. Huang, X. Lu, C-60-Decorated nickel-cobalt phosphide as an efficient and robust electrocatalyst for hydrogen evolution reaction, *Nanoscale*, 10 (2018) 23070-23079.
- [S7] H.G. Liang, C. Yang, S. Ji, N.Y. Jiang, X.F. An, X.W. Yang, H. Wang, R.F. Wang, Cobalt-nickel phosphides@carbon spheres as highly efficient and stable electrocatalyst for hydrogen evolution reaction, *Catalysis Communications*, 124 (2019) 1-5.